Supporting Information

Biomass-Derived Hard Carbon Anodes with Enhanced Capacity for Sodium-Ion Batteries

Huahua Zeng[a#], Juntao He[a#], Jinlian Zhang[a], Qinxuan Zeng[a,b], Ning Li[c], Ming Sun[a,b]*, Lin Yu[a,b]

[a]Guangdong Engineering Technology Research Center of Modern Fine Chemical Engineering, Guangdong Provincial Key Laboratory of Plant Resources Biorefinery, School of Chemical Engineering and Light Industry, Guangdong University of Technology, Guangzhou 510006, China

[b]Jieyang Branch of Chemistry and Chemical Engineering Guangdong Laboratory (Rongjiang Laboratory), Jieyang 515200, China

[c]College of Chemical Engineering, Guangdong University of Petrochemical Technology, Maoming 525000, China

# these two authors contributed equally

*To whom correspondence should be addressed: sunmgz@gdut.edu.cn;

1. Experimental

1.1Physical Characterization

Thermogravimetric analysis (TG Perkin Elmer) was performed to obtain the thermal stability data of the materials. The morphological features of the materials were observed using scanning electron microscopy (SEM, Phenom-world) and Higher resolution transmission electron microscopy (HRTEM, FEI Thermo). Specific surface area and other parameters were determined by nitrogen adsorption-desorption analysis (Quantachrome ASiQwin). The crystalline structure of the materials was investigated using X-ray diffraction (XRD Cu Kα, λ = 1.54056 Å) and Raman spectroscopy (Rman LabRam HR Evolution). X-ray photoelectron spectroscopy (XPS Thermo Fisher) was employed to analyze the surface elemental composition of the materials. The total nitrogen content in both LHC and NLHC were measured by Organic

Element Analyzer (German, Elementar UNICUBE).

1.2 Electrochemical test

1.2.1 Half-Cell Performance Test

The electrochemical performance of the active materials was evaluated using CR2032 coin cells. The active material and polyvinylidene fluoride (PVDF) were mixed in a mass ratio of 8:2 and dispersed in N-methylpyrrolidone (NMP) to form a homogeneous slurry. The slurry was uniformly coated on carbon-coated aluminum foil using a spatula and then dried in a vacuum drying chamber at 60 °C for 12 h (The active mass loading in the electrode sheet is *ca.* 2 mg cm^{-2}). The coated foil was cut into circular electrodes with a diameter of 10 mm. Sodium metal was used as the counter electrode, and a glass fiber membrane (Whatman GF/D) served as the separator. The electrolyte was 1 M NaPF6 in diglyme. The coin cells were assembled in an argon-filled glovebox (H_2O < 0.1 ppm, O_2 < 0.1 ppm). Cyclic voltammetry (CV) and electrochemical impedance spectroscopy (EIS) measurements were conducted using a CHI electrochemical workstation. Galvanostatic charge-discharge (GCD) testing, rate performance testing, long-term cycling testing, and galvanostatic intermittent titration technique (GITT) testing were performed using a LAND CT2001A battery testing system.

1.2.2 Full-Cell Performance Test

Negative electrode preparation: The active material and polyvinylidene fluoride (PVDF) were mixed in a mass ratio of 8:2 and dispersed in NMP to form a homogeneous slurry. The slurry was uniformly coated on copper foil using a spatula and dried in a vacuum drying chamber at 60 °C for 12 h. The coated foil was cut into circular negative electrodes with a diameter of 10 mm. Sodium metal was used as the counter electrode to assemble CR2032 coin cells, and the negative electrode was activated by cycling at 30 mA g^{-1} for 3 cycles. After activation, the negative electrode was removed from the coin cell in the glovebox and stored for later use.

Positive electrode preparation: Commercial $Na_3V_2(PO_4)_3$ (NVP) was used as the active material for the positive electrode. NVP and PVDF were mixed in a mass ratio

of 8:2, and an appropriate amount of NMP was added and ground for 1 h to form a viscous, particle-free slurry. The slurry was uniformly coated on aluminum foil using a spatula and dried in a convective drying oven at 60 °C. The electrode was then cut into circular positive electrodes with a diameter of 14 mm and further dried in a vacuum drying chamber at 60 °C for 12 h.

The CR2032 coin cell was assembled in the following order: negative electrode casing, negative electrode, electrolyte, GF/D separator, electrolyte, positive electrode, spacer, spring, and positive electrode casing. The electrolyte used was 1 M NaPF6 in diglyme.

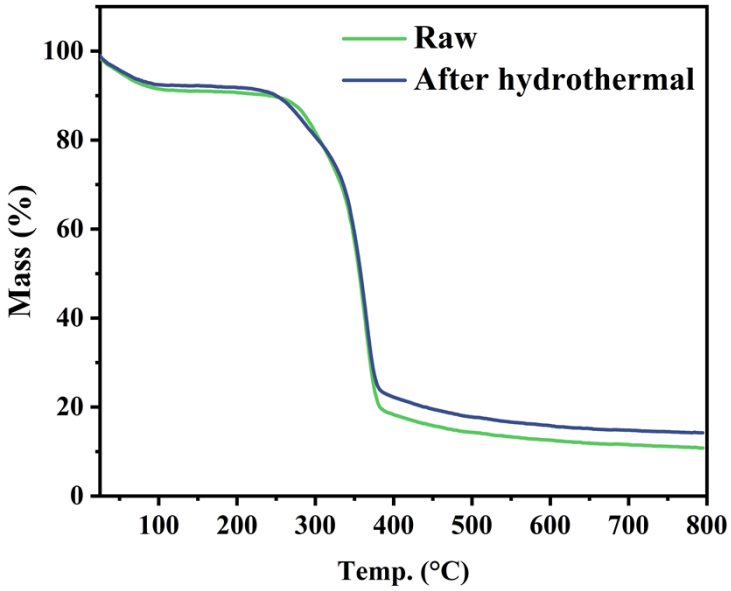

Fig.S1 The TG curves of fresh and hydrothermal treated loofah

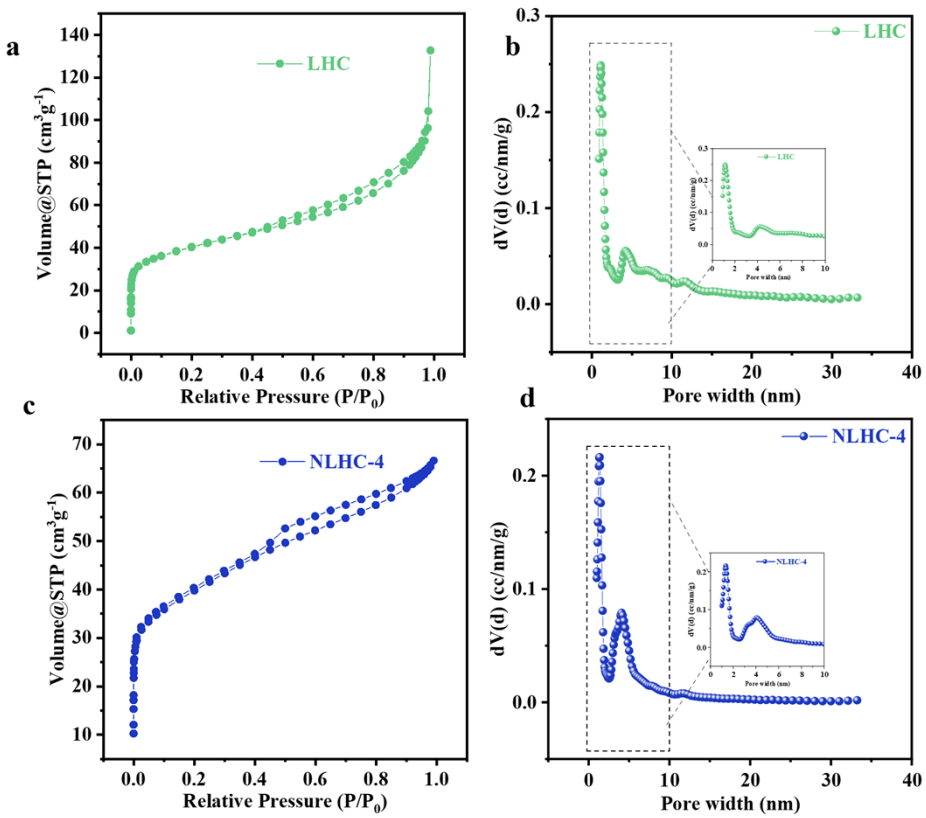

Fig.S2 the absorption and desorption curves of (a) LHC and(b) NLHC； the pore size distributions of (c) LHC and (d) NLHC

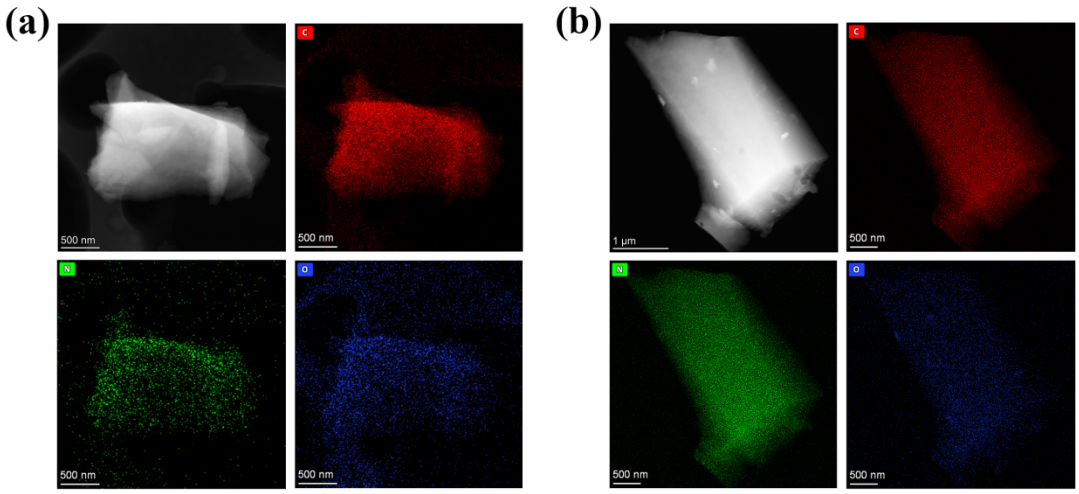

Fig.S3 the element distribution of (a) LHC and (b) NLHC

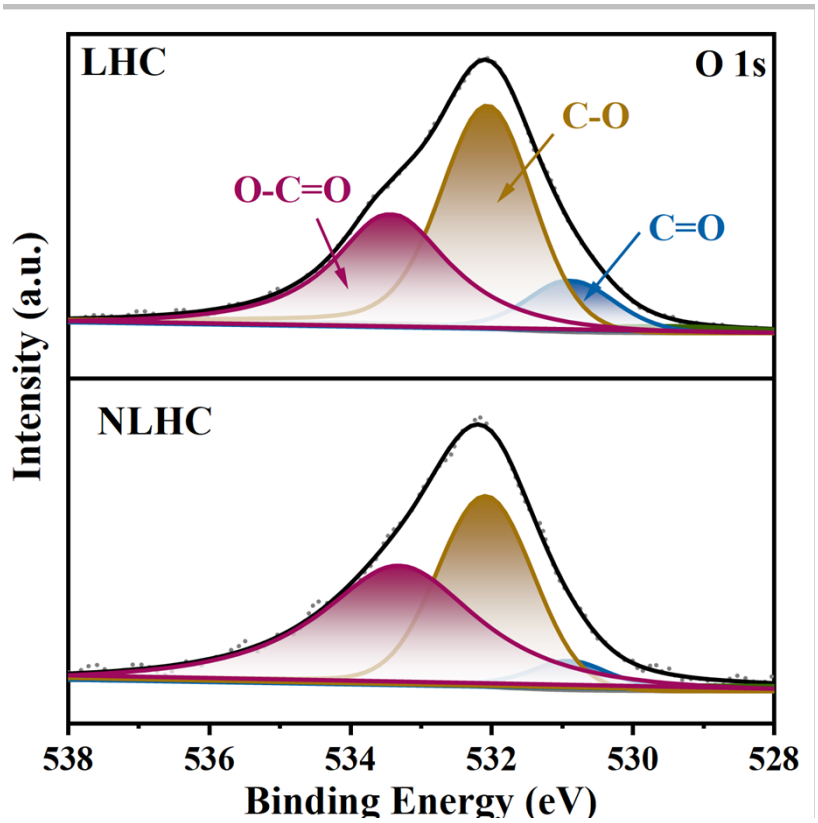

Fig.S4 O1s spectra of LHC and NLHC

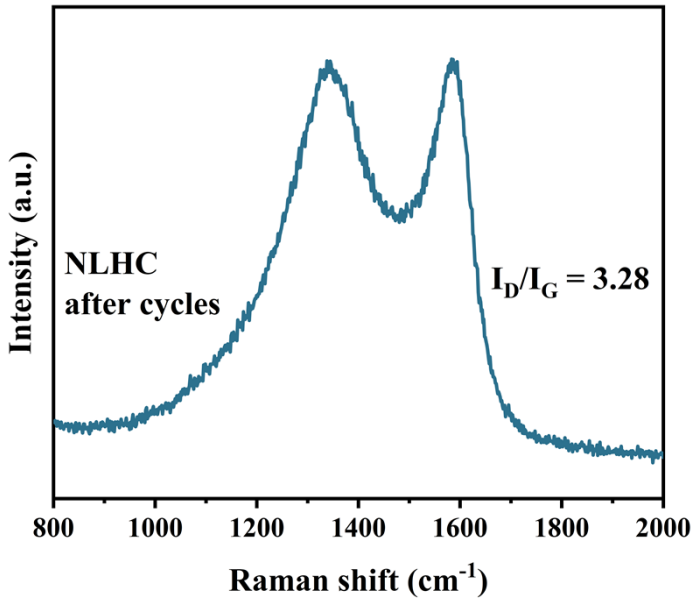

Fig.S5 the Raman of spectra of NLHC after cycling

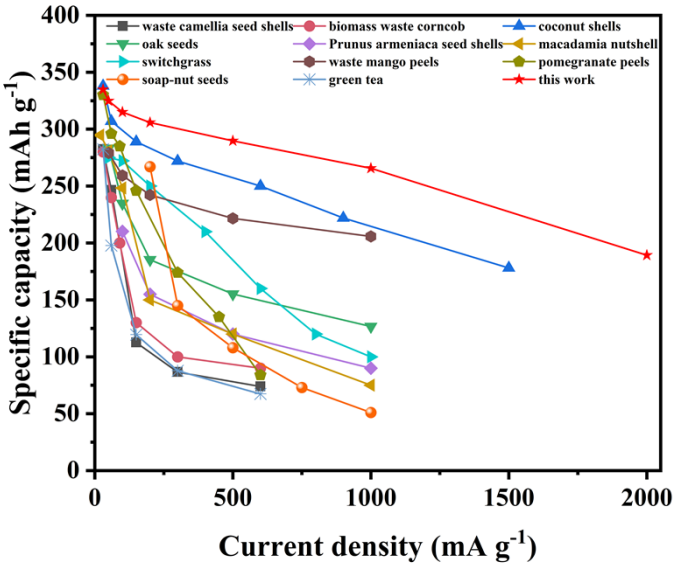

Fig.S6 Reported specific capacities of biomass-derived hard carbon materials for sodium-ion storage.

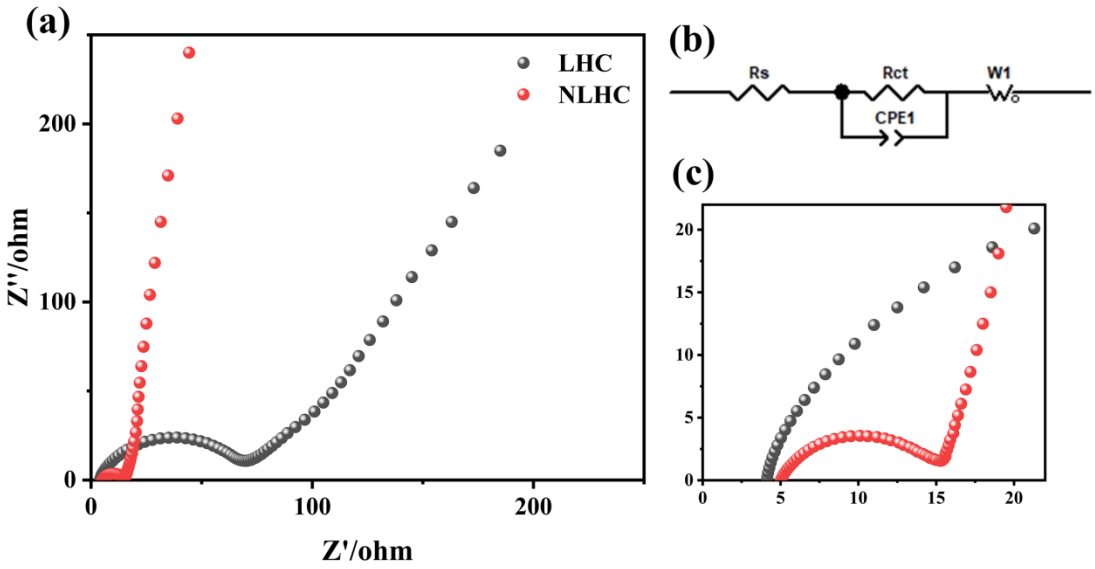

Fig. S7 the EIS curves of (a) LHC and NLHC；(b) the simulated circuit diagram；(c) enlarged EIS curves

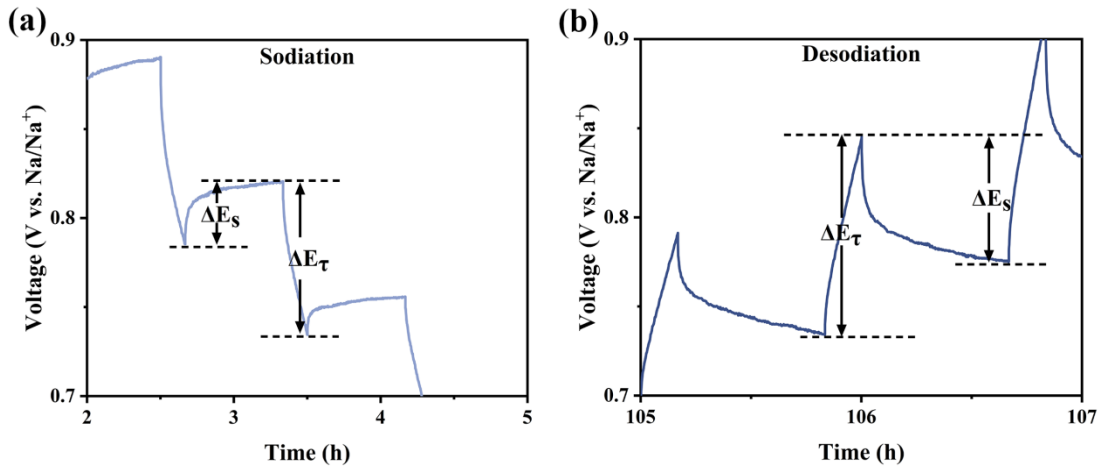

Fig. S8 the obtained ΔE_S and ΔE_τ from GITT curves

Table S1 the impurity of K^+ and Ca^{2+} ions in the carbon materials tested by ICP

	LHC	NLHC-2	NLHC-3	NLHC-4	NLHC-6
K^+	1340.785	1098.646	1074.834	924.305	905.694
Ca^{2+}	35375.46	3969.183	2826.447	1720.256	820.673

Noted：(1) the unit is mg/Kg. (2) NLHC-X, the X means the concentration of NH_4Cl is X mol/L.

Table S2 the surface element content of LHC and NLHC by EDS and total nitrogen content analysis

Sample	C(at%)	O(at%)	N(at%)*	N(%)#
LHC	93.09	6.55	0.36	0.39
NLHC	90.18	8.96	0.86	0.47

Noted: *tested by EDS. #tested by total nitrogen content analysis

Table S3. Sodium storage performance of previously reported biomass-derived hard carbon materials

Precursor	Treatment	Carbonization	Current density (mA g^{-1})	Specific capacity (mAh g^{-1})	ICE(%)	Ref.
waste camellia seed shells	pre-carbonized at 600 ℃ for 2 h; immersed and stirred in 2 M HCl for 6 h	pyrolyzed at 1200, 1300 or 1400 ℃ for 2 h in Ar flow	30	282.4	80.1	[1]
			60	246.5		
			150	112.5		
			300	86.6		
			600	73.9		
			30	270 after 200 cycles		
biomass waste corncob	carbonization at 500 °C for 2 h under an Ar airflow; treated successively with 2 M HCl, 2 M NaOH, and 5% HF; wash till pH=7	heated to 1150, 1300, 1450 °C for 2 h under Ar airflow	30	280	79.6	[2]
			60	240		
			90	200		
			150	130		
			300	100		
			600	90		
			30	250 after 100 cycles		
coconut	carbonization at	calcined at 300	30	338	69.8	[3]

shells	1300 ℃; powder was mixed thoroughly with urea by ball milling at 300 rpm for 5 h	℃ for 2 h in an argon atmosphere	60	307		
			150	289		
			300	272		
			600	250		
			900	222		
			1500	178		
			600	199 after 300 cycles		
oak seeds	immersed in a certain concentration of 15% HF for 12 h after carbonization	carbonization at 1300 ℃ for 6 h	50	283.2	less than 30	[4]
			100	234.7		
			200	185.3		
			500	155.2		
			1000	126.7		
			1000	119.9 after 1000 cycles		
Prunus armeniaca seed shells	pulverized to a partical size of 74 μm	carbonization at 1000, 1100 or 1200 ℃ for 5 h under N_2 flow	100	210.2	not found	[5]
			200	about 155		
			500	about 120		
			1000	about 90		
macadamia nutshell	add macadamia nutshell into a solution of lactic acid and betaine; stirred for hours; washed and dried	carbonization at 1100 ℃ for 2 h	20	294.78	62.36	[6]
			50	281.06		
			100	248.38		
			200	about 150		
			500	about 120		
			1000	about 75		
			100	below 250 after 200 cycles		
switchgrass	grind switchgrass to 1mm powders; hydrothermal treatment at 220 ℃ for 12 h	carbonized at 1600 ℃	50	about 275	84.8	[7]
			100	272.2		
			200	about 250		
			400	about 210		
			600	about 160		
			800	about 120		
			1000	under 100		
			100	308.4 after 100 cycles		
waste mango peels	dried and ground to powders;	calcined at 1000 ℃ for 2 h	50	279.13	70.39	[8]
			100	259.30		

	dispersed in deionized water; hydrothermal treatment at 200 ℃ for 24 h; washed by 1 M HCl		200	242.17	
			500	221.63	
			1000	205.82	
			1000	250.35 after 1000 cycles	
pomegranate peels	washed by HCl and HF after carbonization	carbonized 900, 1000, 1100, 1200 or 1300 ℃	30	330	44.8 [9]
			60	296	
			90	about 285	
			150	246	
			300	174	
			450	about 135	
			600	84	
			150	175 after 200 cycles	
soap-nut seeds	carbonized at 500 ℃ under N_2; planetary milling at 600 rpm for 8 h; washed by HCl and DI water; dried at 100 ℃ overnight	pyrolyzed at 600, 700, 800 or 900 ℃ under N_2	200	267	26.79 [10]
			300	145	
			500	108	
			750	73	
			1000	51	
			300	83 after 500 cycles	
green tea	soaked in 100 ℃ DI water; dried; ground to powder; washed 1 M HCl for 5 h at 60 ℃	carbonized at 1000, 1200, 1400 and 1600 ℃	30	282.4	69 [11]
			60	197.7	
			150	119.4	
			300	87.7	
			600	67.3	
			100	205 after 100 cycles	
this work	hydrothermal treatment in 4 M NH_4Cl	carbonized at 1300 ℃ for 2 h under Ar gas	30	334.8	71.92 /
			50	324.9	
			100	315	
			200	305.8	
			500	289.8	
			1000	265.7	
			2000	189.2	

		1000	191.3 after 1000 cycles

Table S4: Reported energy density or cycle performance of full cells of sodium-ion batteries based on hard carbon

Precursor	**Cathode**	**energy density**	**Reference**
Porphyra	$Na_3V_2(PO_4)_3$@C	69.4 mAh g^{-1} at 100 mA g^{-1} after 100 cycles	[12]
Hard carbon（Merck group）	$Na_3V_2(PO_4)_2F_3$	352.49 Wh kg^{-1}	[13]
Spent Coffee Grounds	$Na_{0.44}MnO_2$	440-490 Wh kg^{-1}	[14]
Waste foam-derived carbon from waste tea, moroccan argan shells, jute silk waste, lotus stem and navel orange peel	$Na_3V_2(PO_4)_3$	205.9 Wh kg^{-1}	[15]
Corn starch	$Na_3V_2(PO_4)_3$	268.81 Wh kg^{-1}	[16]
Corn stover	$NaNi_{1/3}Fe_{1/3}Mn_{1/3}O_2$	118 mAh g^{-1} at 80 mA g^{-1}	[17]
Waste *Camellia semiserrata* shell	$NaFe_{1/3}Ni_{1/3}Mn_{1/3}O_2$	150 mAh g^{-1} at 500 mA g^{-1} after 100 cycles	[18]
Olive shells	$Na_2Fe(Fe(CN)_6)$	320 mAh g^{-1} at 50 mA g^{-1}	[19]
Pomegranate peel	$Na_3V_2(PO_4)_3$	110 mAh g^{-1} at 40 mA g^{-1}	[20]
This work	$Na_3V_2(PO_4)_3$	101.2 mAh g^{-1} at 500 mA g^{-1} after 200 cycles	/

References

[1] Peng J, Tan H, Tang Y, et al. The induced formation and regulation of closed-pore structure for biomass hard carbon as anode in sodium-ion batteries [J]. Journal of Energy Storage, 2024.

[2] Tang Y, He J, Peng J, et al. Electrochemical Behavior of the Biomass Hard Carbon Derived from Waste Corncob as a Sodium-Ion Battery Anode [J]. Energy & Fuels, 2024.

[3] Xiang J, Ma L, Sun Y, et al. Ball-Milling-Assisted N/O Codoping for Enhanced Sodium Storage Performance of Coconut-Shell-Derived Hard Carbon Anodes in Sodium-Ion Batteries [J]. Langmuir, 2024.

[4] Ding J, Zhang Y, Huang Y, et al. Sulfur and phosphorus co-doped hard carbon derived from oak seeds enabled reversible sodium spheres filling and plating for ultra-stable sodium storage [J]. Journal of Alloys and Compounds, 2021.

[5] Oktay Z M, Onal Y, Depci T, et al. Investigation of electrochemical performance of Na-ion batteries by hard carbon anodes produced by biomass of Prunus armeniaca seeds [J]. Journal of Materials Science: Materials in Electronics, 2023.

[6] Wang Q, Du L, Wang S, et al. Biomass-Derived Hard Carbon Anodes Processed with Deep Eutectic Solvents for High-Performance Sodium-Ion Batteries [J]. ACS Omega, 2025.

[7] Li Y, Xia D, Tao L, et al. Hydrothermally Assisted Conversion of Switchgrass into Hard Carbon as Anode Materials for Sodium-Ion Batteries [J]. ACS Applied Materials & Interfaces, 2024.

[8] Liu J, Zhang Z, Yin Y, et al. A mango peel-derived hard carbon as high-performance anode material for sodium-ion batteries [J]. Journal of Industrial and Engineering Chemistry, 2025.

[9] Wu Q, Shu K, Zhao L, et al. Pomegranate Peel-Derived Hard Carbons as Anode Materials for Sodium-Ion Batteries [J/OL] 2024, 29(19).

[10] Khatua S, Achary K R, Rao Y B, et al. Physicochemical activation of soap-nut seeds-derived hard carbon as a sustainable anode for lithium-ion batteries [J]. New Journal of Chemistry, 2024.

[11] Pei L, Cao H, Yang L, et al. Hard carbon derived from waste tea biomass as high-performance anode material for sodium-ion batteries [J]. Ionics, 2020.

[12] Hu X, Fan X, Mou Z, et al. Controlled synthesis of multi-doped highly-disordered porous biomass carbon microsphere for ultra-stable and fast sodium storage [J]. Journal of Energy Storage, 2024.

[13] Mahato S, Das A, Biswas K. Experimental and theoretical investigation on boron, phosphorus dual doped hard carbon as anode for sodium-ion battery [J]. Journal of Energy Storage, 2024.

[14] Pianta N, Florenzano D A, Lorenzi R, et al. Hard Carbon Derived from Spent Coffee Grounds for Applications in Sodium Ions Batteries [J]. Advanced Sustainable Systems, 2025.

[15] Chen Y, Sun H, He X X, et al. Pre-Oxidation Strategy Transforming Waste Foam to Hard Carbon Anodes for Boosting Sodium Storage Performance [J]. Small, 2023.

[16] Zhong H, Huang Q, Zou M, et al. From food to hard carbon: Citric acid enhanced biomass-derived anodes for high-performance sodium storage [J]. Chemical Engineering Journal, 2025.

[17] Wang Y, Li M, Zhang Y, et al. Defect-rich hard carbon designed by heteroatom escape assists sodium storage performance for sodium-ion batteries [J]. Chemical Engineering Journal, 2024.

[18] Huang J, Zhang Q, Yuan M, et al. A distinctive edge-graphited hard carbon for advanced sodium-ion batteries [J]. Journal of Materials Chemistry A, 2025.

[19] Zhou L, Cui Y, Niu P, et al. Biomass-derived hard carbon material for high-capacity sodium-ion battery anode through structure regulation [J]. Carbon, 2025.

[20] Wu Q, Shu K, Zhao L, et al. Pomegranate Peel-Derived Hard Carbons as Anode Materials for Sodium-Ion Batteries [J]. Molecules, 2024.